COBEM2015

ABCM Associação Brasileira de Engenharia e Ciências Mecânicas

23rd ABCM International Congress of Mechanical Engineering
December 6-11, 2015, Rio de Janeiro, RJ, Brazil

Waypoint-Based Guidance with Obstacle Avoidance for Multirotor Vehicles Using a Model Predictive Controller

Davi Antônio dos Santos
Igor Afonso Acampora Prado
José Agnelo Bezerra

Instituto Tecnológico de Aeronáutica
davists@ita.br
igoracampora@gmail.com
agnelo.bgs@gmail.com

Abstract. *This paper deals with the problem of waypoint-based guidance of multirotor aerial vehicles with avoidance of a single polytopic obstacle. In order to solve the problem, a receding horizon model predictive controller (MPC) is adopted. The command inputs to the controller consist of a sequence of tridimensional waypoints as well as a reference speed. The future reference output trajectory embedded in the MPC is chosen as a straight line, traveled with the reference speed, towards the next waypoint of the sequence. A waypoint is detected as soon as the vehicle enters inside a specified Euclidian ball centered at it. At the same moment, the next waypoint of the sequence is switched on. This rule is repeated until reaching the final waypoint, at which the vehicle is commanded to stay. In order to avoid a single polytopic obstacle, a very simple method based on both the previous and the next waypoints is proposed for obtaining a convex optimization space that does not contain the obstacle. The proposed method is evaluated by simulations, showing that it is effective to guide a multirotor vehicle throughout the waypoints, with approximately the reference speed, even in the presence of an obstacle and force disturbances.*

Keywords: *Model Predictive Control, Waypoint Navigation, Multirotor Aerial Vehicles, Obstacle Avoidance*

1. INTRODUCTION

Many papers have investigated the waypoint-based guidance, however considering autonomous vehicles other than the multirotor helicopters; for example, conventional helicopters, airplanes, and farm tractor (Petersen *et al.*, 2013; Lenain *et al.*, 2006; Almeida, 2008; Bousson and Machado, 2013; Richards and How, 2002). Particularly, (Kim *et al.*, 2008) proposed a real-time path planning for an Unmanned Aerial Vehicle (UAV) considering a hostile environment. Two algorithms were designed, in which use extremely limited information of the probabilistic risk in the surrounding with respect to the UAV current position and produce a series of safe waypoints whose rish is almost less than a given threshold value. On the other hand, few works have treated the subject with particular focus on multirotor vehicles and, therefore, there is a large space for contribution in this topic. We could cite one paper dedicated to multirotor vehicles: Nagaty *et al.* (2013). This reference utilized a nonlinear control technique to solve the multirotor trajectory tracking problem. In this paper, the outer loop controller generates the reference trajectories for the inner loop controller to reach the desired waypoint.

The model predictive control (MPC) strategy has proven quite suitable for both trajectory planning and guidance of aerial vehicles (Richards and How, 2002; Almeida, 2008), since it can carry out those tasks in an optimal sense, while considering the existence of constraints on position, velocity, and acceleration. Reference (Richards and How, 2002) tackled the problem of 2D trajectory planning with collision avoidance using Mixed Integer Linear Programming (MILP). In this method, the optimization process automatically decides the order of waypoints to be visited by the vehicle as well as its best trajectory from an initial to a final point, so as to minimize the time to complete the maneuver while respecting speed, force, and obstacle position constraints. The paper (Almeida, 2008) investigates the constrained infinite horizon model predictive control approach in a tridimensional waypoint navigation problem, considering flight and engine limitations.

The present paper proposes a receding horizon model predictive controller (MPC) for tridimensional waypoint-based guidance of multirotor aerial vehicles under thrust force and position constraints in an environment containing a single

[1]This work received financial support from FAPESP (grant 2015/04393-2) and CNPq (grant 475251/2013-0).

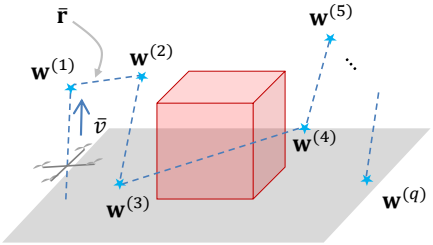

Figure 1. A waypoint-based reference trajectory in an environment containing a polytopic obstacle.

polytopic obstacle. The command inputs to the controller consist of a sequence of tridimensional waypoints as well as a reference speed. The future reference output trajectory embedded in the MPC is chosen as a straight line, traveled with the reference speed, towards the next waypoint of the sequence. The arrival to a waypoint is detected as soon as the vehicle enters inside a specified Euclidian ball centered at it (waypoint detection ball). At the same moment, the next waypoint of the sequence is switched on. This rule is repeated until reaching the final waypoint of the sequence, where the vehicle is commanded to standstill. In order to avoid the obstacle, a very simple method based on both the previous and the next waypoint is proposed for obtaining a convex optimization space that does not contain the obstacle. The proposed method is evaluated by simulations, which shows that it is effective to guide a multirotor vehicle throughout the waypoints, with approximately the reference speed, even in the presence of an obstacle and force disturbances. The remaining text is organized in the following manner. Section 2 enunciates the waypoint-based multirotor guidance problem. Section 3 presents an MPC for solving the guidance problem defined in Section 2. Section 4 shows the simulation results. Finally, Section 5 presents the concluding remarks.

2. PROBLEM DEFINITION

Consider the multirotor aerial vehicle and the three Cartesian coordinate systems (CCS). The body CCS $S_{\mathrm{B}} = \{X_{\mathrm{B}}, Y_{\mathrm{B}}, Z_{\mathrm{B}}\}$ is fixed on the structure of the vehicle at its center of mass (CM). The ground CCS $S_{\mathrm{G}} = \{X_{\mathrm{G}}, Y_{\mathrm{G}}, Z_{\mathrm{G}}\}$ is fixed on the ground at a known point O. The reference CCS $S_{\mathrm{R}} = \{X_{\mathrm{R}}, Y_{\mathrm{R}}, Z_{\mathrm{R}}\}$ is parallel to S_{G}, but its origin is translated to CM. For simplicity, the time dependence of all vectors that will appear from now on in the text will not be denoted explicitly.

Assume that S_{G} is an inertial frame. In this case, an immediate application of the second Newton's law gives the following dynamics model for the translational motion of the vehicle represented in S_{G}:

$$\ddot{\mathbf{r}}_{\mathrm{G}} = \frac{1}{m}\left(\mathbf{f}^{\mathrm{c}}_{\mathrm{G}} + \mathbf{f}^{\mathrm{d}}_{\mathrm{G}}\right) + \mathbf{g}_{\mathrm{G}}, \tag{1}$$

$$\mathbf{f}^{\mathrm{c}}_{\mathrm{G}} = \mathbf{D}^{\mathrm{T}}\mathbf{f}^{\mathrm{c}}_{\mathrm{B}}, \tag{2}$$

where $\mathbf{r}_{\mathrm{G}} \in \mathbb{R}^3$ denotes the position $\mathbf{r}$ of CM represented in S_{G}; $\mathbf{f}^{\mathrm{c}}_{\mathrm{G}}, \mathbf{f}^{\mathrm{c}}_{\mathrm{B}} \in \mathbb{R}^3$ are the total thrust force vector $\mathbf{f}^{\mathrm{c}}$ represented in S_{G} and S_{B}, respectively; $\mathbf{f}^{\mathrm{d}}_{\mathrm{G}} \in \mathbb{R}^3$ is the disturbance force vector $\mathbf{f}^{\mathrm{d}}$ represented in S_{G}; $\mathbf{g}_{\mathrm{G}} \triangleq \begin{bmatrix} 0 & 0 & -g \end{bmatrix}^{\mathrm{T}}$ is the gravitational acceleration vector represented in S_{G}, with g denoting its magnitude; m is the mass of the vehicle; and $\mathbf{D} \in SO(3)$ is the attitude matrix representing the attitude of S_{B} w.r.t. S_{R} (or, equivalently, S_{G}).

Define the jth waypoint $\mathbf{w}^{(j)} \in \mathbb{R}^3$ as a position vector represented in S_{G}. Assume that a sequence $\left\{\mathbf{w}^{(1)}, \mathbf{w}^{(2)}, ..., \mathbf{w}^{(q)}\right\}$ of q waypoints is known beforehand. Consider the specification of a reference speed $\bar{v} \in \mathbb{R}_+$ for the vehicle's trajectory. Therefore, define the reference trajectory $\bar{\mathbf{r}}$ of the vehicle's translational motion as the sequence of line segments linking the waypoints, traveled with speed $\bar{v}$. See the illustration in Figure 1.

Assume that the vehicle is restricted to fly inside a bounded environment described by

$$\mathbf{r}_{\min} \leq \mathbf{r}_{\mathrm{G}} \leq \mathbf{r}_{\max}, \tag{3}$$

where $\mathbf{r}_{\min}, \mathbf{r}_{\max} \in \mathbb{R}^3$ are given limiting positions. Furthermore, consider that this environment contains a single polytopic obstacle, which can be described by (see Figure 2)

$$\boldsymbol{\Theta}\check{\mathbf{r}} \leq \boldsymbol{\theta}, \tag{4}$$

with $\boldsymbol{\Theta} \in \mathbb{R}^{n_s \times 3}$, $\boldsymbol{\theta} \in \mathbb{R}^{n_s}$, where n_s is the number of sides of the obstacle and $\check{\mathbf{r}}$ is a generic position vector satisfying the environment described by (3).

In order to respect the maximal thrust limit of the rotors, avoid inadvertent flips, and maintain all the rotors rotating without stopping, consider the following thrust force constraints:

$$\mathbf{f}_{\min} \leq \mathbf{f}^{\mathrm{c}}_{\mathrm{G}} \leq \mathbf{f}_{\max}, \tag{5}$$

where $\mathbf{f}_{\min}, \mathbf{f}_{\max} \in \mathbb{R}^3$ are given limiting thrust forces. For more details about position control under thrust constraints, see the reference (Santos *et al.*, 2013).

Problem 1. The waypoint-based guidance problem for multirotor aerial vehicles is to find a feedback control law for $\mathbf{f}_{\mathrm{G}}^{\mathrm{c}}$ that makes the vehicle's position $\mathbf{r}_{\mathrm{G}}$ follow the reference trajectory $\bar{\mathbf{r}}$, while respecting the constraints given in (3) and (5) and avoiding the obstacle given in (4) . □

3. PROBLEM SOLUTION

This section presents a solution to Problem 1 based on a incremental state-space formulation of MPC [see (Maciejowski, 2002)].

3.1 Preliminary Considerations

The method presented in this section considers the following two assumptions.

Assumption 1. In the design of the controller, the force disturbances will not be considered.

Assumption 2. Let $\bar{\mathbf{f}} \in \mathbb{R}^3$ denote the thrust command computed by the guidance law defined in Problem 1. Assume that $\mathbf{f}_{\mathrm{G}}^{\mathrm{c}} \equiv \bar{\mathbf{f}}$.

Considering Assumptions 1-2, a design model can be immediately obtained from equation (1) as:

$$\ddot{\mathbf{r}}_{\mathrm{G}} = \frac{1}{m}\bar{\mathbf{f}} + \mathbf{g}_{\mathrm{G}}. \tag{6}$$

3.2 State-Space Model and Constraints

Define the state vector $\mathbf{x} \triangleq \left[\mathbf{r}_{\mathrm{G}}^{\mathrm{T}}\ \dot{\mathbf{r}}_{\mathrm{G}}^{\mathrm{T}}\right]^{\mathrm{T}}$, the controlled output vector $\mathbf{y} \triangleq \mathbf{r}_{\mathrm{G}}$, and the control input vector

$$\mathbf{u} \triangleq \frac{1}{m}\mathbf{f}_{\mathrm{G}}^{\mathrm{c}} + \mathbf{g}_{\mathrm{G}}. \tag{7}$$

From equations (6), (7), one can describe the translational dynamics of the vehicle by the following discrete-time linear time-invariant state-space model:

$$\mathbf{x}_{k+1} = \mathbf{A}\mathbf{x}_k + \mathbf{B}\mathbf{u}_k, \tag{8}$$

$$\mathbf{y}_{k+1} = \mathbf{C}\mathbf{x}_{k+1}, \tag{9}$$

with

$$\mathbf{A} \triangleq \begin{bmatrix} 1 & 0 & 0 & T & 0 & 0 \\ 0 & 1 & 0 & 0 & T & 0 \\ 0 & 0 & 1 & 0 & 0 & T \\ 0 & 0 & 0 & 1 & 0 & 0 \\ 0 & 0 & 0 & 0 & 1 & 0 \\ 0 & 0 & 0 & 0 & 0 & 1 \end{bmatrix}, \mathbf{B} \triangleq \begin{bmatrix} T^2/2 & 0 & 0 \\ 0 & T^2/2 & 0 \\ 0 & 0 & T^2/2 \\ T & 0 & 0 \\ 0 & T & 0 \\ 0 & 0 & T \end{bmatrix} \text{ and } \mathbf{C} \triangleq \begin{bmatrix} 1 & 0 & 0 & 0 & 0 & 0 \\ 0 & 1 & 0 & 0 & 0 & 0 \\ 0 & 0 & 1 & 0 & 0 & 0 \end{bmatrix}, \tag{10}$$

where T is the sampling period.

To ensure robustness to constant disturbances in the control variable, we implement the model at equation (7) in the velocity form (Maciejowski (2002)). Then define the augmented state vector as $\mathbf{z}_k \triangleq \left[\Delta\mathbf{x}_k^{\mathrm{T}}\ \mathbf{y}_k^{\mathrm{T}}\right]^{\mathrm{T}} \in \mathbb{R}^9$, where $\Delta\mathbf{x}_k \triangleq \mathbf{x}_k - \mathbf{x}_{k-1}$.

Using the state $\mathbf{z}_k$, the incremental state-space model can be obtained by algebraic manipulations:

$$\mathbf{z}_{k+1} = \tilde{\mathbf{A}}\mathbf{z}_k + \tilde{\mathbf{B}}\Delta\mathbf{u}_k, \tag{11}$$

$$\mathbf{y}_{k+1} = \tilde{\mathbf{C}}\mathbf{z}_{k+1}, \tag{12}$$

where $\Delta\mathbf{u}_k \triangleq \mathbf{u}_k - \mathbf{u}_{k-1}$ and

$$\tilde{\mathbf{A}} \triangleq \begin{bmatrix} \mathbf{A} & \mathbf{0}_{6\times 3} \\ \mathbf{CA} & \mathbf{I}_3 \end{bmatrix} \in \mathbb{R}^{9\times 9}, \tilde{\mathbf{B}} \triangleq \begin{bmatrix} \mathbf{B} \\ \mathbf{CB} \end{bmatrix} \in \mathbb{R}^{9\times 3}, \tilde{\mathbf{C}} \triangleq \begin{bmatrix} \mathbf{0}_{3\times 6} & \mathbf{I}_3 \end{bmatrix} \in \mathbb{R}^{3\times 9}. \tag{13}$$

From the definition of $\mathbf{y}$, the constraint given in (3) can be rewritten as

$$\mathbf{r}_{\min} \leq \mathbf{y}_k \leq \mathbf{r}_{\max}. \tag{14}$$

Now, using Assumption 2 and equation (7), the constraint given in (5) can be written in terms of $\mathbf{u}_k$, resulting

$$\mathbf{u}_{\min} \leq \mathbf{u}_k \leq \mathbf{u}_{\max}, \tag{15}$$

where $\mathbf{u}_{\min}$ and $\mathbf{u}_{\max}$ are computed using equation (7), but replacing $\bar{\mathbf{f}}$ by $\mathbf{f}_{\min}$ and $\mathbf{f}_{\max}$, respectively.

3.3 Obstacle Avoidance

In order to avoid the obstacle described by (4), we propose the following strategy:

1. Define the obstacle perception radius $\beta \in \mathbb{R}_+$ as a design parameter. To account for the obstacle, we establish the condition

$$d_k^* \leq \beta, \text{ where } d_k^* = \min_{\boldsymbol{\Theta}\check{\mathbf{r}} \leq \boldsymbol{\theta}} \|\check{\mathbf{r}} - \mathbf{r}_k\|. \tag{16}$$

   If the condition of (16) is not verified, the obstacle is simply ignored.

2. Consider that the next waypoint of the sequence is $\mathbf{w}^{(j)}$ and the current time instant is k. Define the ith external side of the obstacle as the set $\mathcal{I}_i \triangleq \{\check{\mathbf{r}} : -\boldsymbol{\Theta}_i \check{\mathbf{r}} \leq -\theta_i\}$, where $\boldsymbol{\Theta}_i$ is the ith line of $\boldsymbol{\Theta}$, and θ_i is the ith component of $\boldsymbol{\theta}$. Then, if at instant k the condition of (16) is verified, for optimization purposes, constrain the flight environment as $\mathcal{I}_i$, for some $i = 1, ..., n_s$ such that $\mathbf{r}_k \in \mathcal{I}_i$ and $\mathbf{w}^{(j)} \in \mathcal{I}_i$, simultaneously.

Supose that the ith obstacle side has been chosen by the above strategy. In this case, using the notation of Section 3.2, the new flight environment is described by

$$-\boldsymbol{\Theta}_i \mathbf{y}_k \leq -\theta_i. \tag{17}$$

3.4 Model Predictive Controller

i. Prediction Model

Denote the prediction horizon by $N \in \mathbb{Z},\ N > 0$ and define the vector of output predicted values along it as

$$\mathbf{Y}_k \triangleq \left[\mathbf{y}_{k+1|k}^{\mathrm{T}}\ \mathbf{y}_{k+2|k}^{\mathrm{T}} \cdots \mathbf{y}_{k+N|k}^{\mathrm{T}}\right]^{\mathrm{T}} \in \mathbb{R}^{3N}. \tag{18}$$

Similarly, define the vector of future incremental inputs at instant k as

$$\Delta\mathbf{U}_k \triangleq \left[\Delta\mathbf{u}_{k|k}^{\mathrm{T}}\ \Delta\mathbf{u}_{k+1|k}^{\mathrm{T}} \cdots \Delta\mathbf{u}_{k+N-1|k}^{\mathrm{T}}\right]^{\mathrm{T}} \in \mathbb{R}^{3N}. \tag{19}$$

As presented in Maciejowski (2002), the prediction model can be obtained from the state-space model in equations (11), (12). So the prediction equation can be written as

$$\mathbf{Y}_k = \mathcal{A}\mathbf{z}_k + \mathcal{B}\Delta\mathbf{U}_k, \tag{20}$$

with

$$\mathcal{A} \triangleq \begin{bmatrix} \tilde{\mathbf{C}}\tilde{\mathbf{A}} \\ \tilde{\mathbf{C}}\tilde{\mathbf{A}}^2 \\ \vdots \\ \tilde{\mathbf{C}}\tilde{\mathbf{A}}^N \end{bmatrix} \in \mathbb{R}^{3N\times 9} \text{ and } \mathcal{B} \triangleq \begin{bmatrix} \tilde{\mathbf{C}}\tilde{\mathbf{B}} & \mathbf{0}_{3\times 3} & \mathbf{0}_{3\times 3} & \cdots & \mathbf{0}_{3\times 3} \\ \tilde{\mathbf{C}}\tilde{\mathbf{A}}\tilde{\mathbf{B}} & \tilde{\mathbf{C}}\tilde{\mathbf{B}} & \mathbf{0}_{3\times 3} & \cdots & \mathbf{0}_{3\times 3} \\ \vdots & & & & \\ \tilde{\mathbf{C}}\tilde{\mathbf{A}}^{N-1}\tilde{\mathbf{B}} & \tilde{\mathbf{C}}\tilde{\mathbf{A}}^{N-2}\tilde{\mathbf{B}} & \tilde{\mathbf{C}}\tilde{\mathbf{A}}^{N-3}\tilde{\mathbf{B}} & \cdots & \tilde{\mathbf{C}}\tilde{\mathbf{B}} \end{bmatrix} \in \mathbb{R}^{3N\times 3N}. \tag{21}$$

ii. Constraints

Applying the constraints (14) and (17) to the predicted outputs $\mathbf{y}_{k+i|k}$, for $i = 1, ..., N$, one can write, respectively,

$$[\mathbf{r}_{\min}]_N \leq \mathbf{Y}_k \leq [\mathbf{r}_{\max}]_N\,, \tag{22}$$

$$-\mathcal{O}\mathbf{Y}_k \leq -\left[\theta_i\right]_N, \tag{23}$$

where $[a]_N$ denotes an extended vector with N copies of a and

$$\mathcal{O} \triangleq \begin{bmatrix} \mathbf{\Theta}_i & \mathbf{0}_{1\times3} & \mathbf{0}_{1\times3} & \dots & \mathbf{0}_{1\times3} \\ \mathbf{0}_{1\times3} & \mathbf{\Theta}_i & \mathbf{0}_{1\times3} & \dots & \mathbf{0}_{1\times3} \\ \vdots & \vdots & \vdots & \dots & \vdots \\ \mathbf{0}_{1\times3} & \mathbf{0}_{1\times3} & \mathbf{0}_{1\times3} & \dots & \mathbf{\Theta}_i \end{bmatrix} \in \mathbb{R}^{N\times3N} \tag{24}$$

Using (20), equations (22) and (23) can be rewritten in terms of $\Delta\mathbf{U}_k$, yielding

$$\left[\mathbf{r}_{\min}\right]_N - \mathcal{A}\mathbf{z}_k \leq \mathcal{B}\Delta\mathbf{U}_k \leq \left[\mathbf{r}_{\max}\right]_N - \mathcal{A}\mathbf{z}_k, \tag{25}$$

$$-\mathcal{O}\mathcal{B}\Delta\mathbf{U}_k \leq -\left[\theta_i\right]_N + \mathcal{O}\mathcal{A}\mathbf{z}_k. \tag{26}$$

It's necessary to write the constraint (15) in terms of $\Delta\mathbf{u}_k$, in order to adjust it to the incremental formulation. From reference (Maciejowski (2002)), we obtain

$$\mathbf{U}_k = \left[\mathbf{u}_{k-1}\right]_N + \mathcal{T}_N\Delta\mathbf{U}_k, \tag{27}$$

where

$$\mathcal{T}_N = \begin{bmatrix} \mathbf{I}_3 & \mathbf{0}_{3\times3} & \dots & \mathbf{0}_{3\times3} \\ \mathbf{I}_3 & \mathbf{I}_3 & \dots & \mathbf{0}_{3\times3} \\ \vdots & \vdots & \dots & \vdots \\ \mathbf{I}_3 & \mathbf{I}_3 & \dots & \mathbf{I}_3 \end{bmatrix} \in \mathbb{R}^{3N\times3N} \text{ and } \mathbf{U}_k \triangleq \begin{bmatrix} \mathbf{u}_{k|k} \\ \mathbf{u}_{k+1|k} \\ \vdots \\ \mathbf{u}_{k+N-1|k} \end{bmatrix} \in \mathbb{R}^{3N}. \tag{28}$$

Applying equation (27) in (15), we have

$$\left[\mathbf{u}_{\min}\right]_N \leq \left[\mathbf{u}_{k-1}\right]_N + \mathcal{T}_N\Delta\mathbf{U}_k \leq \left[\mathbf{u}_{\max}\right]_N, \tag{29}$$

Finally, equations (25), (26) and (29) can be immediately put into the form

$$\mathbf{\Xi}\Delta\mathbf{U}_k \leq \boldsymbol{\xi}, \tag{30}$$

with

$$\mathbf{\Xi} \triangleq \begin{bmatrix} \mathcal{B} \\ -\mathcal{B} \\ -\mathcal{O}\mathcal{B} \\ \mathcal{T}_N \\ -\mathcal{T}_N \end{bmatrix} \in \mathbb{R}^{13N\times3N} \text{ and } \boldsymbol{\xi} \triangleq \begin{bmatrix} \left[\mathbf{r}_{\max}\right]_N - \mathcal{A}\mathbf{z}_k \\ -\left[\mathbf{r}_{\min}\right]_N + \mathcal{A}\mathbf{z}_k \\ -\left[\theta_i\right]_N + \mathcal{O}\mathcal{A}\mathbf{z}_k \\ \left[\mathbf{u}_{\max} - \mathbf{u}_{k-1}\right]_N \\ -\left[\mathbf{u}_{\min} - \mathbf{u}_{k-1}\right]_N \end{bmatrix} \in \mathbb{R}^{13N}. \tag{31}$$

iii. Future Trajectory

Denote the future reference trajectory for $\mathbf{Y}_k$ by

$$\bar{\mathbf{Y}}_k \triangleq \left[\bar{\mathbf{y}}_{k+1|k}^{\mathrm{T}}\, \bar{\mathbf{y}}_{k+2|k}^{\mathrm{T}} \cdots \bar{\mathbf{y}}_{k+N|k}^{\mathrm{T}}\right]^{\mathrm{T}}, \tag{32}$$

where, for $i = 1, ..., N$, $\bar{\mathbf{y}}_{k+i|k}$ denotes the reference value for $\mathbf{y}_{k+i|k}$.

Suppose that, at instant k, the current waypoint is $\mathbf{w}^{(j)}$. In order to command the vehicle to follow a straight line towards $\mathbf{w}^{(j)}$, with a speed command $\bar{v}$, we adopt

$$\bar{\mathbf{y}}_{k+i|k} = \bar{\mathbf{y}}_{k+i-1|k} + \frac{\mathbf{w}^{(j)} - \bar{\mathbf{y}}_{k|k}}{\|\mathbf{w}^{(j)} - \bar{\mathbf{y}}_{k|k}\|}\bar{v}T, \tag{33}$$

for $i = 1, ..., N$ and $\bar{\mathbf{y}}_{k|k} \triangleq \tilde{\mathbf{C}}\mathbf{z}_k$. Note that the second term of the right-hand side of (33) is the product of a reference velocity vector with a time step. Moreover, one can see that the reference velocity has a magnitude $\bar{v}$ and points towards the direction of the current waypoint $\mathbf{w}^{(j)}$.

It is not interesting that the reference trajectory overshoots the waypoint $\mathbf{w}^{(j)}$. So, for a $\bar{\mathbf{y}}_{k+i|k}$ calculated as equation (33) such that

$$\|\bar{\mathbf{y}}_{k+i|k} - \bar{\mathbf{y}}_{k|k}\| > \|\mathbf{w}^{(j)} - \bar{\mathbf{y}}_{k|k}\|, \tag{34}$$

we impose that $\bar{\mathbf{y}}_{k+i|k} = \mathbf{w}^{(j)}$.

An exception to the trajectory of equation (33) occurs when the vehicle reaches the final waypoint $\mathbf{w}^{(q)}$. In this case, it is commanded to stay at $\mathbf{w}^{(q)}$ by simply making $\bar{\mathbf{y}}_{k+i|k} = \mathbf{w}^{(q)}$, for $i = 1, ..., N$.

iv. Waypoint Commutation

For switching from the current waypoint $\mathbf{w}^{(j)}$ to the next one $\mathbf{w}^{(j+1)}$ of the waypoint sequence, we adopt the following rule. Let the system be initialized with the first waypoint $\mathbf{w}^{(1)}$ as the current one. Suppose now that at a certain instant k, the waypoint $\mathbf{w}^{(j)}$ is the current one. Define the waypoint detection ball $\mathcal{B}_{\mathbf{w}^{(j)}}(\lambda) \subset \mathbb{R}^3$ as being an Euclidian ball centered at $\mathbf{w}^{(j)}$, with a radius λ. From now on, $\lambda \in \mathbb{R}$ is called the waypoint detection radius. Therefore, the commutation to the next waypoint $\mathbf{w}^{(j+1)}$ of the waypoint sequence is realized, up to the last waypoint $\mathbf{w}^{(q)}$, as soon as

$$\mathbf{y}_k \in \mathcal{B}_{\mathbf{w}^{(j)}}(\lambda) \tag{35}$$

is verified.

v. Computation of the Control Input

The optimal incremental input vector $\Delta\mathbf{u}_k^*$ consists of the first three elements of $\Delta\mathbf{U}_k$ that minimizes the quadratic cost functional

$$\mathcal{J}(\Delta\mathbf{U}_k) = \|\mathbf{Y}_k - \bar{\mathbf{Y}}_k\|^2 + \rho\|\Delta\mathbf{U}_k\|^2, \tag{36}$$

subject to the constraints in equation (30), where $\rho \in \mathbb{R},\ \rho > 0$ is a design weighting parameter. Then, the optimal control input vector $\mathbf{u}_k^*$ is obtained by $\mathbf{u}_k^* = \mathbf{u}_{k-1} + \Delta\mathbf{u}_k^*$.

The above problem can be immediately put into the format of a conventional quadratic optimization problem under linear inequality constraints. To solve this convex optimization problem, efficient numerical methods are available (Boyd and Vandenberghe, 2004).

vi. Computation of the Force Magnitude and Attitude Commands

As soon as the control input vector $\mathbf{u}_k^*$ is computed, it can be converted into the corresponding thrust command $\bar{\mathbf{f}}_k$ by using equation (7). However, this force command is not sufficient as an output of a guidance law for a multirotor aerial vehicle. In fact, the system has to provide two commands for the vehicle's internal control loops: a command for the magnitude of the total thrust vector and an attitude command. The complete explanation to understand how the controller compute these informations can be found in Prado and Santos (2014).

4. SIMULATION RESULTS

This section aims to evaluate the proposed guidance method using computational simulations. Subsection 4.1 describes the simulation environment, while Subsection 4.2 presents the results and comments.

4.1 System Simulation

The proposed guidance system was simulated in MATLAB/Simulink with a six-degree-of-freedom dynamics model of attitude and position, considering a quadrotor in "plus" configuration with the following parameters: mass $m = 1$ kg, inertia matrix $J = \mathrm{diag}\{0.02, 0.02, 0.03\}$ kg m^2, frame radius $l = 0.2$ m, time constant of the motor-drive $\tau = 0.01$ s, maximum speed of the motor $\omega_{\max} = 10^4$ rpm, force constant of the rotor $k_f = 3.13 \times 10^{-5}$ N/(rad/s)^2 and moment constant of the rotor $k_t = 7,5 \times 10^{-7}$ N m/(rad/s)^2. In the (internal) attitude control loop, a saturated proportional-derivative control law with proportional gain $K_p = 20$ and derivative gain $K_d = 8$ is used. On the other hand, in the (external) position control loop, the MPC proposed in Section 3 is adopted. Table 2 presents the controller parameters used in the simulations. From the values of $\mathbf{f}_{\min}$ and $\mathbf{f}_{\max}$, one can compute the maximum inclination command as $\bar{\varphi}_{\max} = 45$ degree, the minimum thrust magnitude command as $\bar{f}_{\min} = 2$ N, and the maximum thrust magnitude command as $\bar{f}_{\max} = 20.05$ N.

The vehicle is considered to fly subject to a constant disturbance force, simulating a light wind. Thus the adopted disturbance force is $\mathbf{f}_{\mathrm{G}}^{\mathrm{d}} = [1\ \ 0\ \ 0]^{\mathrm{T}}$ N. The disturbance torque is neglected, for simplicity. The polytopic obstacle described

Table 1. Parameters of the MPC controller.

Parameter	**Value**
Prediction horizon	$N = 20$
Sampling time	$T = 0.1$ s
Control weight	$\rho = 20$
Reference speed	$\bar{v} \in \{3.0, 4.0, 5.0\}$ m/s
Obstacle perception radius	$\beta \in \{0, 0.1, 0.5, 1.0\}$ m
Minimum position	$\mathbf{r}_{\min} = [-5 \ -5 \ -5]^{\mathrm{T}}$ m
Maximum position	$\mathbf{r}_{\max} = [50 \ 50 \ 50]^{\mathrm{T}}$ m
Minimum thrust	$\mathbf{f}_{\min} = [-1 \ -1 \ 2]^{\mathrm{T}}$ N
Maximum thrust	$\mathbf{f}_{\max} = [1 \ 1 \ 20]^{\mathrm{T}}$ N

by (4) is chosen with

$$\boldsymbol{\Theta} = \begin{bmatrix} 1 & 0 & 0 \\ -1 & 0 & 0 \\ 0 & 1 & 0 \\ 0 & -1 & 0 \\ 0 & 0 & 1 \\ 0 & 0 & -1 \end{bmatrix}, \quad \boldsymbol{\theta} = \begin{bmatrix} 16 \\ -6 \\ 16 \\ -6 \\ 10 \\ 0 \end{bmatrix}.$$

4.2 Results and Comments

Two trajectories containing four waypoints are chosen. The waypoints in the first trajectory are: $\mathbf{w}^{(1)} = [\ 0 \quad 0 \quad 0\ ]^{\mathrm{T}}$, $\mathbf{w}^{(2)} = [\ 8 \quad 1 \quad 5\ ]^{\mathrm{T}}$ m, $\mathbf{w}^{(3)} = [\ 8 \quad 5 \quad 5\ ]^{\mathrm{T}}$ m and $\mathbf{w}^{(4)} = [\ 25 \quad 5 \quad 5\ ]^{\mathrm{T}}$ m, while the second trajectory in composed by the following waypoints $\mathbf{w}^{(1)} = [\ 9 \quad 8 \quad 16\ ]^{\mathrm{T}}$ m, $\mathbf{w}^{(2)} = [\ 12 \quad 11 \quad 16\ ]^{\mathrm{T}}$ m, $\mathbf{w}^{(3)} = [\ 12 \quad 11 \quad 10.5\ ]^{\mathrm{T}}$ m and $\mathbf{w}^{(4)} = [\ 20 \quad 11 \quad 10.5\ ]^{\mathrm{T}}$ m, as illustrated in Figures 2-3, respectively. In order to evaluate the proposed method, the trajectory reference speed $\bar{v}$ and the obstacle detection radius β are varied to assume the values specified in Table 1.

Figure 2 shows the first vehicle's trajectory together with the reference trajectory. The first column presents the results without obstacle deviation, which corresponds to the vehicle trajectory in a hypothetical space without the obstacle. In this case, the solid green lines show that the vehicle would enter into the obstacle. However, increasing the parameter β, one can see that the vehicle is able to realize the polytope so that the obstacle constraints are activated and the controller optimizes the trajectory to avoid it. When the speed $\bar{v}$ is increased up to 4.0 m/s, the vehicle is not able to avoid the obstacle, considering $\beta = 0.1$ m. It happens because the multirotor helicopter only "sees" the polytope at a short distance such that it cannot produce the lateral deceleration required to avoid the cube. This scenario also occurs when $\bar{v}$ goes up to 5.0 m/s. In these two aforementioned cases, when the parameter β is increased, the vehicle can deviate of the obstacle because the multirotor helicopter "sees" it from a larger distance, allowing the controller to implement a turn in the path.

Figure 3 presents the vehicle behavior during a vertical approach to the obstacle. As shown in the previews cases, the vehicle enters into the solid when the obstacle deviation algorithm is not implemented. However, for the smaller value of the obstacle perception radius, the quadrotor only shocks with the cube for the higher speed. In the scenario with $\bar{v} = 4$ m/s and $\beta = 0.1$ m, one can see that the vehicle is able to deviate from the solid. In comparison with the first trajectory, the aerial vehicle has more capability to avoid the obstacle in this case. It is justified due to the rotors capability to produce bigger thrust in the Z_G direction (see Table 1).

Finally, is possible to see that the disturbance force doesn't affect so much the vehicle's path, once it can pass by all the waypoints even in the worst cases. This fact proves the model's robustness to constant disturbance at inputs.

5. CONCLUSIONS

The present paper proposed a model predictive controller (MPC) for waypoint-based guidance with obstacle avoidance of multirotor aerial vehicles. The commands to the controller are a sequence of waypoints and a reference speed. The proposed method is able to guide the vehicle along a desired trajectory respecting a set of linear constraints. These ones are activated when the obstacle enters into the perception sphere.

The simulations showed that the vehicle entered into the obstacle region when the obstacle algorithm was not enabled. However, by increasing the parameter β, the vehicle was able to avoid the cube. So, the method's efficiency was verified.

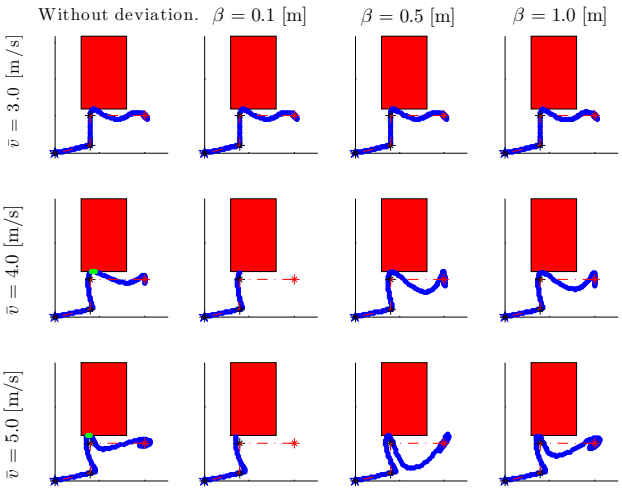

Figure 2. Considering the $X_G - Y_G$ plane, the solid blue lines represent the trajectory of the vehicle. The red rectangle is the obstacle. The solid green lines are the vehicle path inside the obstacle when the obstacle avoidance is not implemented. The dashed lines represent the reference trajectory and the stars represent the waypoints. The red star is the last waypoint.

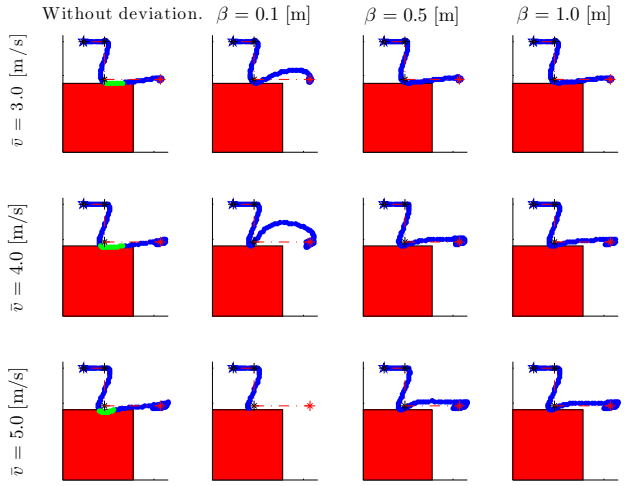

Figure 3. Considering $X_G - Z_G$ plane. The descriptions are the same as used in Figure 2.

6. REFERENCES

Almeida, F., 2008. "Waypoint navigation using constrained infinite horizon model predictive control". In *AIAA Guidance, Navigation and Control Conference and Exhibit*. Honolulu, Hawaii.

Bousson, K. and Machado, P.F.F., 2013. "4d trajectory generation and tracking for waypoint-based aerial navigation". *WSEAS Transactions on Systems and Control*, Vol. 3, No. 8, pp. 105–119.

Boyd, S. and Vandenberghe, L., 2004. *Convex Optimization*. Cambridge University Press, New York.

Kim, Y., Gu, D.W. and Postlethwaite, I., 2008. "Real-time path planning with limited information for autonomous unmanned air vehicles". *Automatica*, Vol. 44, No. 8, pp. 696–712.

Lenain, R., Thuilot, B., Cariou, C. and Martinet, P., 2006. "High accuracy path tracking for vehicles in presence of sliding: Application to farm vehicle automatic guidance for agricultural tasks". *Autonomous Robots*, Vol. 21, pp. 79–97.

Maciejowski, J.M., 2002. *Predictive Control with Constraints*. Harlow: Prentice Hall.

Nagaty, A., Saeedi, S., Thibault, C., Seto, M. and Li, H., 2013. "Control and navigation framework for quadrotor helicopters". *Journal of Intelligent and Robotic Systems*, Vol. 70, No. 8, pp. 1–12.

Petersen, C., Baldwin, M. and Kolmanovsky, I., 2013. "Model predictive control guidance with extended command governor inner-loop flight control for hypersonic vehicles". In *AIAA Guidance, Navigation, and Control (GNC) Conference*. Boston, USA.

Prado, I.A.A. and Santos, D.A., 2014. "A safe position tracking strategy for multirotor helicopters". In *22st Mediterranean Conference on Control and Automation*. Palermo, Italy.

Richards, A. and How, J.P., 2002. "Aircraft trajectory planning with collision avoidance using mixed integer linear programming". In *Proceedings of the American Control Conference*. Anchorage, USA.

Santos, D.A., Saotome, O. and Cela, A., 2013. "Trajectory control of multirotor helicopters with thrust vector constraints". In *21st Mediterranean Conference on Control and Automation*. Platanias, Greece.

7. RESPONSIBILITY NOTICE

The authors are the only responsible for the printed material included in this paper.